Computational Study of Turbulent Laminar Patterns in Couette Flow

Dwight Barkley*
Mathematics Institute, University of Warwick, Coventry CV4 7AL, United Kingdom

Laurette S. Tuckerman†
LIMSI-CNRS, BP 133, 91403 Orsay, France

(Received 29 March 2004; published 7 January 2005)

Turbulent-laminar patterns near transition are simulated in plane Couette flow using an extension of the minimal-flow-unit methodology. Computational domains are of minimal size in two directions but large in the third. The long direction can be tilted at any prescribed angle to the streamwise direction. Three types of patterned states are found and studied: periodic, localized, and intermittent. These correspond closely to observations in large-aspect-ratio experiments.

DOI: 10.1103/PhysRevLett.94.014502 PACS numbers: 47.20.–k, 47.27.–i, 47.54.+r, 47.60.+i

Plane Couette flow—the flow between two infinite parallel plates moving in opposite directions—undergoes a discontinuous transition from laminar flow to turbulence as the Reynolds number is increased. Because of its simplicity, this flow has long served as one of the canonical examples for understanding shear turbulence and the subcritical transition process typical of channel and pipe flows [1–11]. Only recently was it discovered in very large-aspect-ratio experiments by Prigent *et al.* [12–14] that this flow also exhibits remarkable pattern formation near transition. Figure 1 shows such a pattern, not from experiment, but from numerical computations reported here. An essentially steady, spatially periodic pattern of distinct regions of turbulent and laminar flow emerges spontaneously from uniform turbulence as the Reynolds number is decreased. The most striking features of these patterns are their large wavelength and the oblique angle they form to the streamwise direction.

Related patterns have a long history in fluid dynamics. In Taylor-Couette flow between counter-rotating cylinders, Coles and van Atta [15–17] first discovered a state known as spiral turbulence with coexisting turbulent and laminar regions. This state was famously commented on by Feynman [18] and has attracted attention as an example of a coherent structure comprising both turbulence and long-range order [19–21]. Until recently all experimental studies of this state showed only one turbulent and one laminar patch. Prigent *et al.* [12–14] found that in a very large-aspect-ratio Taylor-Couette system, the turbulent and laminar regions form a periodic pattern, of which the original observations of Coles comprised only one wavelength. Cros and Le Gal [22] discovered large-scale turbulent spirals as well, in experiments on the shear flow between a stationary and a rotating disk. The Reynolds-number thresholds, wavelengths, and angles are very similar for all of these turbulent patterned flows. It now appears that such patterns are inevitable intermediate states on the route from turbulent to laminar flow in large-aspect-ratio shear flows.

We report the first direct numerical simulation of turbulent-laminar patterns. Our simulations are designed to reduce computational expense, to establish minimal conditions necessary to produce these large-scale patterns, and to impose and thereby investigate the pattern wavelength and orientation. To do so, we use tilted rectangular domains which are long perpendicular to the turbulent bands, allowing for pattern formation and wavelength competition, and of minimal size along the bands, in which the pattern is homogeneous, the flow varying only over the small scales typical of shear turbulence; see Fig. 1.

In plane Couette flow, plates located at $y = \pm h$ move at velocities $\pm U\hat{\mathbf{x}}$. The Reynolds number is $\mathrm{Re} = hU/\nu$, where ν is the fluid's kinematic viscosity. We take $h = 1$,

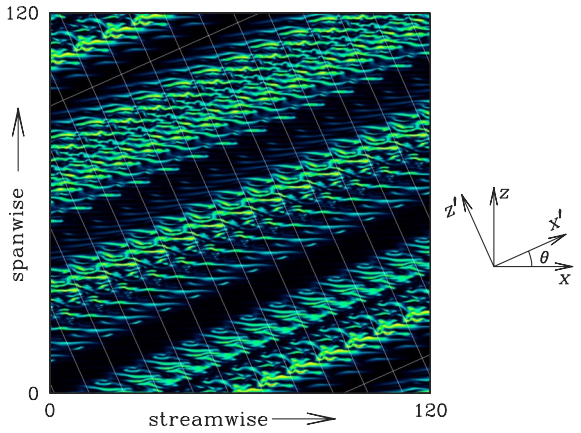

FIG. 1 (color online). Turbulent-laminar pattern at Reynolds number 350. The computational domain (outlined in white, aligned along x', z') is repeated periodically to tile an extended region. The kinetic energy is visualized in a plane midway between and parallel to the plates moving in the streamwise (x) direction. Uniform black corresponds to laminar flow. The sides of the image are 60 times the plate separation $L_y = 2$; the pattern wavelength is 20 L_y. Streamwise streaks, with spanwise extent approximately L_y, are visible at the edges of the turbulent regions.

$U = 1$. The simple Couette solution $\mathbf{u_C} \equiv y\hat{\mathbf{x}}$ is linearly stable for all values of Re. However, above a critical Re near 325 [6], transition to turbulence occurs for sufficiently large perturbations. The turbulence is characterized by the cyclical generation and breakdown of streaks by streamwise-oriented vortices with a natural spanwise pair spacing of about 4 [1,5,7,9,23,24]. In minimal-flow-unit (MFU) simulations [1,5,9], a periodic domain of minimal lateral dimensions is sought which can sustain this basic cycle. For plane Couette flow near transition, the minimum size is approximately $L_x \times L_z = 6 \times 4$ [Fig. 2(a)].

We extend the MFU computations in two ways. First we tilt the domain at angle θ to the streamwise direction [Fig. 2(b)], designating by x' and z' the periodic directions of the tilted domain. To respect the spanwise streak spacing while imposing periodic boundary conditions in x', the domain satisfies $L_{x'} \sin\theta \simeq 4$ for $\theta > 0$. (For $\theta = 0$, we require $L_{x'} \gtrsim 6$.) Second, we greatly extend one of the dimensions $L_{z'}$ past the MFU requirement [Fig. 2(c)], in practice between 30 and 220, usually 120.

The incompressible Navier-Stokes equations are simulated using a spectral-element ($x' - y$)–Fourier (z') code [25]. The boundary conditions are no-slip at the moving plates and periodic in the x' and z' directions. The spatial resolution for the $L_{x'} \times L_y \times L_{z'} = 10 \times 2 \times 120$ domain is $N_x \times N_y \times N_z = 61 \times 31 \times 1024$, consistent with previous studies [5,9]. We have verified the accuracy of our simulations in small domains by comparing to prior simulations [5]. In large domains we have examined mean velocities, Reynolds stresses, and correlations in a turbulent-laminar flow at Re = 350 and find that these reproduce experimental results from Taylor-Couette [17] and plane Couette [7] flow. While neither experimental study corresponds exactly to our case, the agreement supports our claim that our large-domain simulations correctly capture turbulent-laminar states.

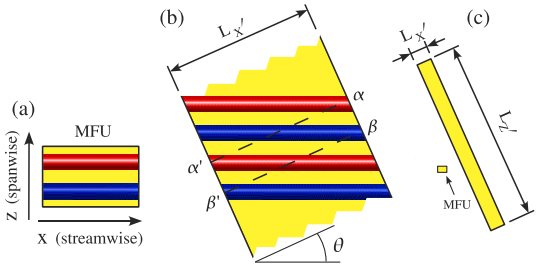

FIG. 2 (color online). Simulation domains. The wall-normal direction y is not seen; $L_y = 2$. The gray or colored bars represent streamwise vortex pairs with a spanwise spacing of 4. (The vortices are schematic; these are dynamic features of the actual flow.) (a) MFU domain of size 6×4. (b) Central portion of a domain [on the same scale as (a)] tilted to the streamwise direction. α, α', and β, β' are pairs of points identified under periodic boundary conditions in x'. (c) Full tilted domain with $L_{x'} = 10$, $L_{z'} = 120$, and $\theta = 24°$. On this scale the MFU domain, shown for comparison, is small.

We make two comments distinguishing our approach. Experimentalists [12–14] vary Re and report the measured angles and wavelengths, varying from $\theta = 25°$ and $\lambda_{z'} = 46$ at Re = 394 to $\theta = 37°$ and $\lambda_{z'} = 60$ at Re = 340. (They extrapolated the domain of existence to be $325 \leq \mathrm{Re} \leq 415$.) In contrast, we fix the pattern angle and restrict the wavelength: in this way, we can determine the boundaries in parameter space within which each pattern can exist. Second, all the turbulent states we report are bistable with simple Couette flow. A major goal [6,8–11], not addressed here, has been the determination of lifetimes and transition probabilities of turbulent flow as a function of amplitude and Re.

We begin with simulations exploring the dependence of patterns on Re. To allow the system sufficient freedom to select different states, we set $L_{z'} = 120$, 2 to 3 times the experimentally observed wavelength. We fix $\theta = 24°$, near its observed value at pattern onset. Figure 3 shows a long simulation over a time $T = 43\,000$ and spanning the range $420 \geq \mathrm{Re} \geq 290$, with Re decreased in discrete steps over time. A space-time diagram of kinetic energy is shown in the middle and spatial Fourier transforms are on the left.

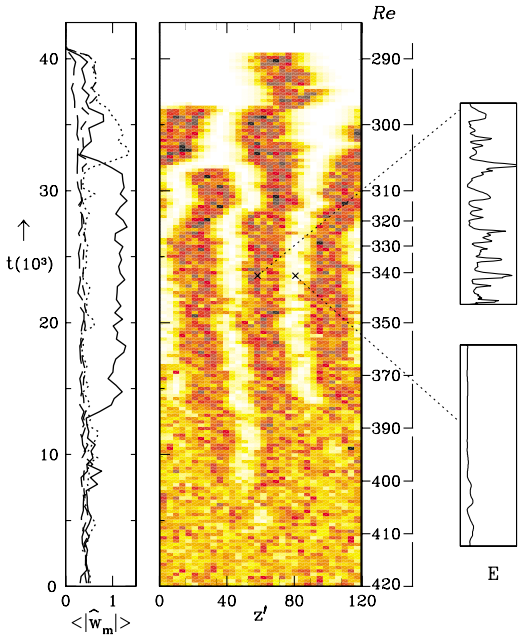

FIG. 3 (color online). Space-time evolution of turbulent-laminar patterns in the domain $L_{x'} \times L_{z'} = 10 \times 120$, $\theta = 24°$. Time evolves upward with changes in Re indicated on the right. States seen upon decreasing Re from uniform turbulence at Re = 420, through various patterned states, ending in simple Couette flow at Re = 290. Center: Time-averaged kinetic energy $\langle E \rangle$ on a space-time grid. The same scale is used for all space-time plots, with $\langle E \rangle = 0$ in white. Right: kinetic energy plotted over a time window $T = 500$ in a turbulent and laminar region. Left: Average spectral components $\langle |\hat{w}_m| \rangle$ of spanwise velocity with $m = 3$ (solid line) and $m = 2$ (dotted line), $m = 0$ (long-dashed line), and $m = 1$ (short-dashed line).

More specifically, we compute $E = |\mathbf{u} - \mathbf{u_C}|^2/2$ at 32 points equally spaced in z' along a line ($x' = y = 0$) in the midchannel and average these time series over windows of length $T = 500$ to yield $\langle E \rangle$, which measures the flow's turbulent intensity on a space-time grid. (Other measures such as the individual velocity components or the rms rather than the means give similar results.) Fig. 3 also shows E from which $\langle E \rangle$ is computed at two points on the space-time grid. We also compute the instantaneous spatial (z') Fourier transform $\hat{w}_m$ of the spanwise velocity w for the same 32 points. We take the modulus (to remove phase information) and average over windows of length $T = 500$ to obtain $\langle |\hat{w}_m| \rangle$; we plot these for $m = 0,1,2$, and 3 on the right. We find that these low-order spectral components of w provide the best diagnostic of pattern wavelength.

We initialized a turbulent flow at Re = 500 by perturbing simple Couette flow and subsequently decreased Re in discrete steps of 10 or 20. Figure 3 begins at Re = 420 with an unpatterned turbulent state we call *uniform turbulence*. Its low-m spectral components $\langle |\hat{w}_m| \rangle$ are all of comparable size. At Re = 410 laminar regions begin to appear and disappear and this continues through Re = 400 (see below). At Re = 390 a stable pattern forms with three distinct turbulent and laminar regions. The $m = 3$ spectral component emerges. The selected wavelength of 40 agrees closely with experiment [12–14]. The final flow at Re = 350 is that visualized in Fig. 1. The pattern remains qualitatively the same through Re = 320. At Re = 310 the pattern loses one turbulent region, accompanied by the emergence of the $m = 2$ spectral component. At Re = 300, a single turbulent region remains, and finally, at Re = 290, the flow reverts to simple Couette flow.

We now present evidence that the patterns in Fig. 3 represent three qualitatively different states. The banded state at Re = 350 is fundamentally *spatially periodic*. To support this we show in Fig. 4 a simulation at Re = 350 in a domain whose length $L_{z'}$ is slowly increased. The pattern adjusts to keep the wavelength in the approximate range 35–65 by splitting the turbulent bands when they grow too large. The instantaneous integrated energy profile $\bar{E} \equiv \int dx'dyE(x', y, z', t)$ is plotted at the final time. Between the turbulent bands, $\bar{E}$ does not reach zero and the flow, while basically laminar, differs from the simple Couette solution $y\mathbf{e_x}$.

In sharp contrast, the single turbulent patch seen in Fig. 3 prior to return to laminar Couette flow is a *localized state*. Figure 4 shows that in a domain of increasing size at Re = 300 a single turbulent region of approximately fixed extent persists, independent of $L_{z'}$. Moreover, $\bar{E}$ decays to zero exponentially as the flow approaches the simple Couette solution away from the patch. The localized states in our computations necessarily take the form of bands when visualized in the $x - z$ plane [e.g., right half of Fig. 5]. Isolated bands and spots are reported experimentally [12–14] near these values of Re.

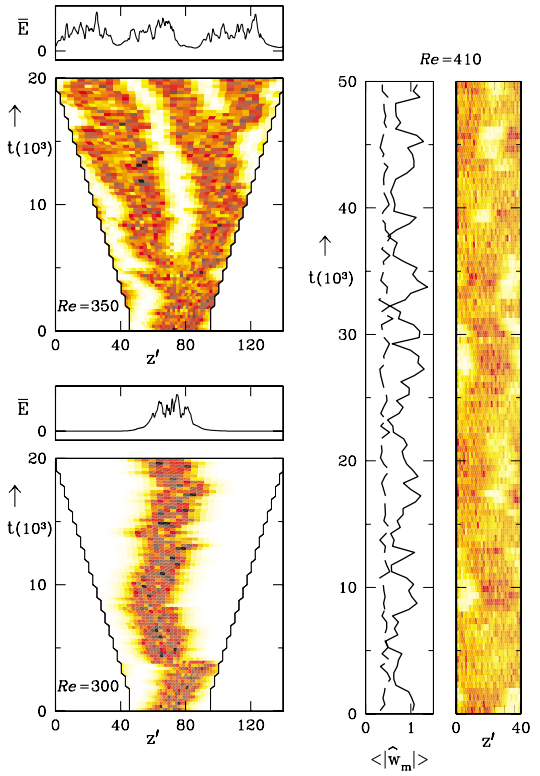

FIG. 4 (color online). Simulations at Re = 350, Re = 300, and Re = 410 illustrating three distinct states: periodic, localized, and intermittent. Space-time representation of $\langle E \rangle$ is as in Fig. 3. For Re = 350 and Re = 300 the domain length is increased from $L_{z'} = 50$ to $L_{z'} = 140$ in increments of 5. The integrated energy profile $\bar{E}(z')$ is shown at the final time. For Re = 410 a single long simulation is shown for $L_{z'} = 40$, accompanied by $m = 1$ (solid line) and $m = 0$ (dashed line) spectral components.

The third behavior is displayed by the *intermittent state* in Fig. 3 near the transition to uniform turbulence. Figure 4 shows a very long simulation at Re = 410 in a domain $L_{z'} = 40$, the size of a single pattern wavelength. The flow never stabilizes but instead quasilaminar regions nucleate and disappear continually. The range of $\langle E \rangle$ in the space-time plot is noticeably smaller than for the stable patterns.

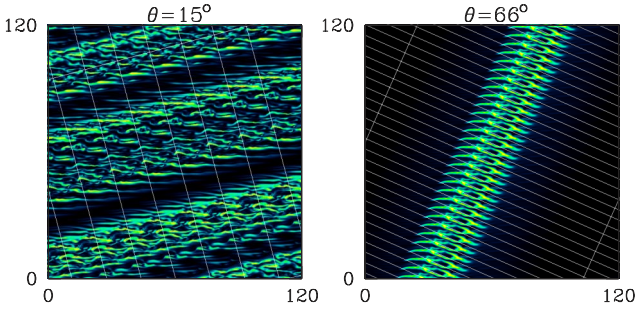

FIG. 5 (color online). Turbulent-laminar patterns at minimum ($\theta = 15°$) and maximum ($\theta = 66°$) angle for which they have been computed at Re = 350. Conventions as in Fig. 1.

Simulations at $L_{z'} = 120$, Re $= 410$ show similar behavior, as do simulations at Re $= 400$ (not immediately evident in Fig. 3 because of the long time scale of the intermittent events). Intermittency has been interpreted in [12–14] as resulting from noise-driven competition between banded patterns at equal and opposite angles. However, the intermittency is captured in our simulations, even though the competition between states of opposite angles is absent.

We have also examined transitions for Re increasing. The transition from banded to intermittent and then to uniform turbulence occurs at the same values of Re, up to our step size of ΔRe $= 10$, as in Fig. 3. (The characteristics of the intermittent state make it difficult to determine the threshold more accurately than this.) Thus there is no or little hysteresis in these transitions. States for Re < 330 are somewhat protocol dependent in that the number of bands at a given Re is not unique.

We have explored regions of existence for various states as a function of Re, wavelength, and tilt. By varying $L_{z'}$ at $\theta = 24°$, Re $= 350$, we have determined that the minimum and maximum wavelengths are approximately 35 and 65, respectively. For $L_{z'} \lesssim 30$, only uniform turbulence is obtained. For $L_{z'} \gtrsim 70$ two bands of wavelength $L_{z'}/2$ form (as in Fig. 4). This range of allowed wavelengths is nearly independent of Re wherever we have computed banded states. Figure 5 shows a banded state at $\theta = 15°$ and a localized state at $\theta = 66°$, the minimum and maximum angles for which we have thus far obtained patterns for $L_{z'} = 120$, Re $= 350$. These extreme states may not be stable without imposed periodicity. The sequence of states seen for increasing θ at Re $= 350$ is qualitatively the same as that for decreasing Re at $\theta = 24°$: $\theta = 0°$ gives uniform turbulence and $\theta = 90°$ simple Couette flow.

In past years minimal-flow-unit simulations have been used to great effect in understanding shear turbulence. We have shown that the same philosophy can be employed in the study of large-scale structures formed in turbulent flows. Specifically, we have reported the first simulations of turbulent-laminar patterns in plane Couette flow by solving the Navier-Stokes equations in domains with a single long direction. The other dimensions are just large enough to resolve the interplate distance and to contain an integer number of longitudinal vortex pairs or streaks. Thus we have demonstrated that the patterns are quasi one-dimensional and we have identified what we believe to be near-minimal conditions necessary for their formation. Key is that the computational domain be tilted obliquely to the streamwise direction of the flow. We have found periodic, localized, and intermittent states where similar states are observed experimentally. We have explored the patterns' dependence on Reynolds number, wavelength, and tilt. Future studies of these states may shed light on the mechanisms responsible for laminar-turbulent patterns and for turbulent transition.

We thank Olivier Dauchot for valuable discussions and Ron Henderson for the use of PRISM. We thank the CNRS and the Royal Society for supporting this work. The two CPU decades of computer time used for this research were provided by the IDRIS-CNRS supercomputing center under project 1119, and by the University of Warwick Centre for Scientific Computing (with support from JREI Grant No. JR00WASTEQ).

*Electronic address: barkley@maths.warwick.ac.uk
URL: www.maths.warwick.ac.uk/~barkley
†Electronic address: laurette@limsi.fr
URL: www.limsi.fr/Individu/laurette

[1] J. Jiménez and P. Moin, J. Fluid Mech. **225**, 213 (1991).
[2] A. Lundbladh and A. V. Johansson, J. Fluid Mech. **229**, 499 (1991).
[3] F. Daviaud, J. Hegseth, and P. Bergé, Phys. Rev. Lett. **69**, 2511 (1992).
[4] N. Tillmark and P. H. Alfredsson, J. Fluid Mech. **235**, 89 (1992).
[5] J. M. Hamilton, J. Kim, and F. Waleffe, J. Fluid Mech. **287**, 317 (1995).
[6] O. Dauchot and F. Daviaud, Phys. Fluids **7**, 335 (1995).
[7] J. J. Hegseth, Phys. Rev. E **54**, 4915 (1996).
[8] A. Schmiegel and B. Eckhardt, Phys. Rev. Lett. **79**, 5250 (1997).
[9] F. Waleffe, Phys. Fluids **15**, 1517 (2003).
[10] B. Hof, A. Juel, and T. Mullin, Phys. Rev. Lett. **91**, 244502 (2003).
[11] H. Faisst and B. Eckhardt, J. Fluid Mech. **504**, 343 (2004).
[12] A. Prigent, Ph.D. thesis, University Paris-Sud, 2001.
[13] A. Prigent, G. Grégoire, H. Chaté, O. Dauchot, and W. van Saarloos, Phys. Rev. Lett. **89**, 014501 (2002).
[14] A. Prigent, G. Grégoire, H. Chaté, and O. Dauchot Physica D (Amsterdam) **174**, 100 (2003).
[15] D. Coles, J. Fluid Mech. **21**, 385 (1965).
[16] C. W. van Atta, J. Fluid Mech. **25**, 495 (1966).
[17] D. Coles and C. W. van Atta, AIAA J. **4**, 1969 (1966).
[18] R. P. Feynman, *Lecture Notes in Physics* (Addison-Wesley, Reading, MA, 1964).
[19] C. D. Andereck, S. S. Liu, and H. L. Swinney, J. Fluid Mech. **164**, 155 (1986).
[20] J. J. Hegseth, C. D. Andereck, F. Hayot, and Y. Pomeau, Phys. Rev. Lett. **62**, 257 (1989).
[21] A. Goharzadeh and I. Mutabazi, Eur. Phys. J. B **19**, 157 (2001).
[22] A. Cros and P. Le Gal, Phys. Fluids **14**, 3755 (2002).
[23] S. Bottin, O. Dauchot, F. Daviaud, and P. Manneville, Phys. Fluids **10**, 2597 (1998).
[24] D. Barkley and L. S. Tuckerman, Phys. Fluids **11**, 1187 (1999).
[25] R. D. Henderson and G. E. Karniadakis, J. Comput. Phys. **122**, 191 (1995).